Thermochimica Acta, 149 (1989) 301–315
Elsevier Science Publishers B.V., Amsterdam – Printed in The Netherlands

APPLICATION OF RIGOROUS NONLINEAR REGRESSION TO THE DECOMPOSITION KINETICS OF EXPLOSIVES

JAMES M. PICKARD
*EG and G Mound * Applied Technologies, Miamisburg, OH 45343-0987 (U.S.A.)*
(Received 2 January 1989)

ABSTRACT

A method based on rigorous nonlinear regression is used to determine global rate parameters for the condensed phase decomposition of an explosive monitored by isothermal differential scanning calorimetry. Nonlinear regression provides relative errors for each global rate parameter, quantitative assessments for the quality of the regression fit, and absolute errors for the resultant Arrhenius parameters. Application of the method is demonstrated for evaluation of global rate parameters for the decomposition of 2,2′,4,4′,6,6′-hexanitroazobenzene(HNAB) at constant volume and constant pressure.

INTRODUCTION

Differential scanning calorimetry (DSC) provides a convenient technique for monitoring the condensed phase decomposition kinetics of secondary explosives. Thermograms for isothermal decomposition of explosives are frequently characterized by non-zero initial rates followed by additional transitions involving autocatalysis. Examples of this phenomenon are illustrated in Fig. 1 for the decomposition of 2,2′,4,4′,6,6′-hexanitroazobenzene (HNAB); both thermograms exhibit nonzero initial rates followed by autocatalytic transitions with maximum rates in the range of 250 to 550 s. In view of the complexity of these thermograms, a computer program using nonlinear regression [1] was devised to evaluate global rate parameters for the condensed phase reactions.

Global reactivity is formally defined as

$$\dot{\alpha} = \sum k_i \Gamma_i f_i(\alpha, P_1, P_2, \ldots P_n) \quad (1)$$

where $\dot{\alpha}$ is the total reaction rate, α is the extent of conversion, and k_i, Γ_i, and $f_i(\alpha, P_1, P_2, \ldots P_n)$ are the rate coefficient, stoichiometric factor, and

* Mound is operated by EG and G Mound Applied Technologies for the U.S. Department of Energy under Contract No. DE-AC04-76-DP43495.

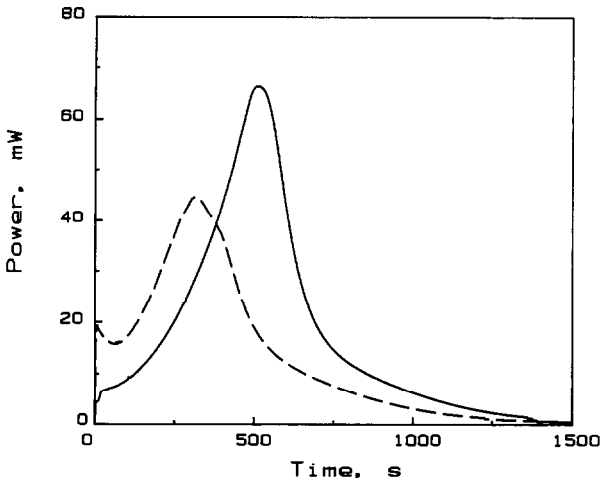

Fig. 1. Thermograms for the isothermal decomposition of HNAB at constant volume: ——, 5.94 mg, 590 K; - - - - - -, 4.13 mg, 600 K.

rate law function defined by the global reaction mechanism from the parameters, P_1, P_2, ... P_n for the ith transition observed in the thermogram [2]. Nonlinear regression based on eqn. (1) offers several advantages over methods [3–7] commonly used to derive global rate parameters, namely, the absence of constraints applied to evaluation of reaction orders, the relative error assessments for each parameter, and the absolute errors for the Arrhenius parameters. With proper weighting of the variables, quantitative statistical tests may be applied in order to assess the quality of the regression fit, and ultimately, the validity of the assumed global reactivity function. This paper describes the application of nonlinear regression for a kinetics analysis of the isothermal decomposition of the explosive HNAB at constant volume and constant pressure over the temperature range 560–633 K.

REGRESSION ALGORITHM

Global rate parameters were determined by the method of undetermined Lagrangian multipliers described in detail by Wentworth [8,9]. Briefly, this algorithm assumes that for N observations of two variables (x, y) and M parameters (k_1, k_2, ... k_M), a condition equation may be expressed as

$$F_i(\bar{x}, \bar{y}, k_1, k_2, \ldots k_M) = 0 \quad i = 1 \text{ to } N \tag{2}$$

where $\bar{x}$ and $\bar{y}$ represent the adjusted or calculated values of the true variables (x, y). Because N is finite, it is impossible to determine the true variables (x, y) and parameters (k_1, k_2, ... k_M); however, estimates may be

obtained by the method of least-squares. The sum of residuals may be expressed as

$$S = \sum \left(W_{xi} V_{xi}^2 + W_{yi} V_{yi}^2 \right) \quad i = 1 \text{ to } N \tag{3}$$

where (W_{xi}, W_{yi}) and (V_{xi}, V_{yi}) are the weight and variance for the ith observation of the independent and dependent variables [8]. Thus, the regression problem reduces to the minimization of S subject to constraints defined by eqn. (2). Weights for each variable are defined from the inverse of the variance (V_{xi} and V_{yi}) as V_0/V_{xi} and V_0/V_{yi} where V_0 is the variance of unit weight.

Expansion of eqn. (2) as a first-order Taylor series with initial values of the parameters $(k_1^{\ominus}, k_2^{\ominus}, \ldots k_M^{\ominus})$, and followed by the introduction of N undetermined multipliers [8,9] led to a system of M linear equations

$$\sum_j \sum_l \sum_i F_{k_{ji}} F_{k_{li}} \delta k_l / L_i = \sum_j \sum_i F_i^{\ominus} F_{k_{ji}} / L_i \quad j = 1 \text{ to } M;$$
$$l = 1 \text{ to } M; \; i = 1 \text{ to } N \tag{4}$$

In eqn. (4), $F_{k_{ji}}$ and $F_{k_{li}}$ are partial derivatives of eqn. (2) with respect to parameters, $k_1, k_2, \ldots k_M$, $L_i = F_{xi}^2/W_{xi} + F_{yi}^2/W_{yi}$, $F_i^{\ominus}$ is an initial estimate of the condition equation, and δk_l are corrections for the initial parameters. L_i is equivalent to $1/W_F$, the weighting parameter employed by algorithms not based on Lagrangian multipliers [8].

The normal equations were solved by iteration for the corrections $(\delta k_1, \delta k_2, \ldots \delta k_M)$ by matrix inversion. New values of the parameters were calculated by subtracting the corrections from the initial estimates. Convergence was checked after each iteration by comparing an estimate of variance with that derived for the preceding iteration. Variance was estimated after each iteration from eqn. (5)

$$\begin{aligned} S = \Big[& \sum \left(F_i^{\ominus 2} \right) / L_i \\ & - \sum \left(F_{k_{1i}} F_i^{\ominus} \delta k_1 \right) / L_i \\ & - \sum \left(F_{k_{2i}} F_i^{\ominus} \delta k_2 \right) / L_i \\ & - \ldots \sum \left(F_{k_{Mi}} F_i^{\ominus} \delta k_M \right) / L_i \Big] / (N - M) \quad i = 1 \text{ to } N \end{aligned} \tag{5}$$

which follows from the use of Lagrangian multipliers in eqn. (2) [8]. Convergence was considered satisfactory if the difference in absolute value of two successive estimates of S was less than $0.01 V_0$.

GLOBAL REACTIVITY AND CONDITION FUNCTIONS

The global reactivity was approximated from a simplified reaction scheme based on analogies to the decomposition of azobenzene [10,11], and a partial

analysis of the HNAB decomposition products.

$$RN{=}NR \rightarrow R\cdot + RN{=}N\cdot \quad \text{(i)}$$

$$RN{=}N\cdot \rightarrow R\cdot + N_2 \quad \text{(ii)}$$

$$RN{=}NR \rightarrow 2R\cdot + N_2 \quad \text{(i + ii)}$$

$$y(R\cdot \text{ or } RN{=}N\cdot) + z\,RN{=}NR \rightarrow \text{products} \quad \text{(iii)}$$

In reactions (i)–(iii), RN=NR is HNAB, R· is a trinitrophenyl radical, and RN=N· is a trinitrophenyldiazenyl radical. In the initial stages of reaction, equilibration of reaction (i) would yield half-order kinetics for HNAB depletion, while the sum, [(i) + (ii)] would lead to first-order kinetics. Stoichiometric coefficients y and z in reaction (iii) correspond to sums for all exothermic bimolecular reactions of HNAB with the intermediate free radicals. Transitions 1 and 2 were assumed to arise solely from the sum, [(i) + (ii)], and the generalized scheme represented by reaction (iii). Therefore, expansion of eqn. (1) assuming x-order kinetics for transition 1 and autocatalysis for transition 2 led to

$$\dot{\alpha} = k_1\Gamma_1(1-\alpha)^x + k_2\Gamma_2\alpha^y(1-\alpha)^z \quad (6)$$

The desired expression for global reactivity was expressed as

$$\alpha = k_1 M_0^{x-1}(1-\alpha)^x + k_2 M_0^{y+z-1}\alpha^y(1-\alpha)^z \quad (7)$$

with Γ_1 and Γ_2 defined from the initial mass, M_0, assuming $M = M_0(1-\alpha)$. The condition equation was defined by rearrangement of eqn. (7)

$$F(\alpha, \dot{\alpha}, k_1, k_2, x, y, z) = k_1 M_0^{x-1}(1-\alpha)^x + k_2 M_0^{y+z-1}\alpha^y(1-\alpha)^z - \dot{\alpha} \quad (8)$$

EXPERIMENTAL

Samples of HNAB obtained from Pantex Corp. were used without additional purification after analysis by high pressure liquid chromatography (HPLC) revealed a purity exceeding 98%. Isothermal decomposition of HNAB under an argon atmosphere at constant pressure and/or constant volume was monitored with a Setaram DSC-111 heat flux calorimeter. Average reactivity curves at constant volume were calculated from a minimum of at least four replicate determinations with sample weights measured with a precision of ±0.01 mg. Total reaction heat, rate, and extent of conversion at each sampling point were calculated from eqns. (9)–(11)

$$Q = \sum (P_i + P_{i+1})F/2 \quad i = 1 \text{ to } N \quad (9)$$

$$\dot{\alpha} = (P_i + P_{i+1})/(2Q) \quad (10)$$

$$\alpha = \sum (P_i + P_{i+1})F/(2Q) \quad (11)$$

where Q is total heat, F is the sampling frequency, and P_i and P_{i+1} are successive observations of the heat flow. The variance of Q and each of the variables (α, $\dot{\alpha}$) were calculated from equations for error propagation [12] derived from eqns. (9)–(11).

The significance of heterogeneous reactions, i.e. the simultaneous occurrence of both condensed and gas phase reactions, was assessed in two ways. First, the volume (≈ 0.15 cm^3) of the DSC crucibles used for constant volume measurements was varied by addition of stainless steel spacers of known volume while maintaining a constant sample mass. The mass/free volume ratio, M/V, was varied within the range of 15–80 mg mm^{-3} in an attempt to minimize the variability associated with the crucible free volume. Secondly, reactions corresponding to a three-fold variation in sample mass ($\approx$ 4–13 mg) were run at a constant pressure of 5×10^6 Pa using Setaram constant pressure crucibles. This approach provided data at a constant pressure by allowing expansion of the product gases from the 0.15 cm^3 sample crucibles into an external 500 cm^3 buffer volume maintained at a pressure of 5×10^6 Pa. Runs in which the sample mass exceeded 13 mg usually resulted in sample deflagration.

The autocatalytic nature of transition 2 observed by DSC was confirmed independently by HPLC analysis. Samples of HNAB aged at 590 K for 1–10 min were periodically analyzed by HPLC in order to determine the extent of reaction. Samples aged for periods of time exceeding 2 min showed an accelerated rate of HNAB depletion, and a multiplicity of unidentified reaction products.

Initial values of the rate parameters were determined as follows. The rate coefficient k_1 was approximated as the initial rate, and the reaction order x was equated to unity. For autocatalytic transitions, the reaction orders and rate coefficient are related by eqns. (12) and (13)

$$\alpha_m = y/(y+z) \tag{12}$$

$$k_2 = \dot{\alpha}_m/\left(M_0^{y+z-1}\alpha_m^y(1-\alpha_m)^z\right) \tag{13}$$

where α_m is the extent of conversion at the maximum rate, $\dot{\alpha}_m$. Initial values for k_2 and y were estimated from eqns. (12) and (13) assuming z equal to unity. In the event that this initial set of parameters resulted in a poor approximation of the global reactivity, the process was repeated by increasing the initial estimate of z by a factor of unity, or by selecting a new set of parameters based on corrections determined in the first few iterations. Slight instabilities were usually observed in the first couple of iterations, even for well-conditioned calculations.

RESULTS AND DISCUSSION

A summary of the number of experiments, sample mass, number of data points, total heat, and standard deviation (σ) for decomposition of HNAB

TABLE 1

Sampling statistics for HNAB decomposition at constant volume [a]

Temperature (K)	No. of runs	No. of data pts./run	Mass (mg)	Q [b] ($J\ g^{-1}$)
633	4	1057	4.24	4527±17
633	5	920	2.52	4791±17
623	4	1028	4.64	4820±13
612	4	1087	2.35	4502±29
600	4	1291	4.13	4682±46
600	5	2798	2.52	5012±13
590	5	1585	5.94	4410±17
590	4	3006	2.93	4820±13
580	6	2866	2.98	4971± 8
570	4	2009	9.02	4883±25
570	4	3315	3.65	5096±17
560	4	2538	9.23	4259±29
560	5	3402	2.89	4561±13

[a] Crucible volume $\approx 0.15\ cm^3$.

[b] Errors correspond to one σ.

at constant volume over the temperature range 560–633 K is given in Table 1. Values of Q are reasonably constant over the whole temperature range. The observed uncertainties for Q are less than 1%.

Plots of the standard deviations for α and $\dot{\alpha}$ versus α for the average global reactivity at 600 K determined at constant volume are illustrated in Fig. 2. Figure 2 indicates that the standard deviation for each observation of α is greater than the corresponding value for $\dot{\alpha}$, and that the largest values

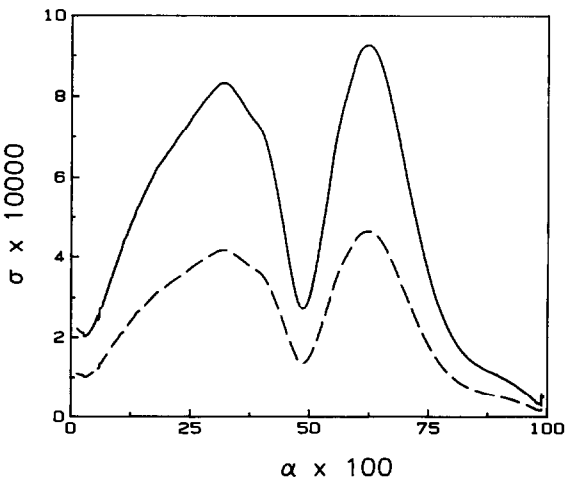

Fig. 2. Standard deviation of α and $\dot{\alpha}$ versus α for decomposition of HNAB at constant volume, 600 K: ------, $\dot{\alpha}$; ——, α.

TABLE 2

Regression data for HNAB decomposition at 600 K

Parameter	Initial	Final [a]
Const. V [b]		
k_1	9.7211×10^{-4}	$(167.7 \pm 4.059)\times10^{-5}$
x	0.5	$(51.41 \pm 1.325)\times10^{-2}$
k_2	3.2328×10^{-2}	$(19.35 \pm 3.408)\times10^{-5}$
y	1.8	2.292 ± 0.1361
z	2.0	2.600 ± 0.1361
Const. P [c]		
k_1	1.677×10^{-4}	$(176.8 \pm 5.172)\times10^{-5}$
x	0.6	$(68.3 \pm 1.287)\times10^{-2}$
k_2	2.725×10^{-5}	$(24.25 \pm 1.331)\times10^{-6}$
y	1.95	1.827 ± 0.0125
z	2.86	2.843 ± 0.0201

[a] Convergence tolerance: 8.58×10^{-9} at const. V, 1×10^{-10} at const. P.
[b] Crucible volume ≈ 0.15 cm^3.
[c] Crucible buffer volume ≈ 500 cm^3, $P = 5\times10^6$ Pa.

occur at $\alpha \approx 62\%$. The data illustrated in Fig. 2 are typical of each reaction temperature in which the largest variance of α and $\dot{\alpha}$ occurred near the maximum rate of the autocatalytic transition.

Therefore, for statistical weighting of data collected at constant volume, V_0 at each reaction temperature was equated to the maximum value of σ_α^2 calculated from error propagation. Unit weighting was assumed for all data collected at constant pressure, and V_0 was assigned a reasonable value of 1×10^{-8}, based on the experience with constant volume measurements.

Representative regression output for data collected at both constant volume and constant pressure at 600 K is given in Table 2. Included in Table 2 are the initial parameters, convergence tolerance, and the final parameters with standard deviations. Standard deviations for the final parameters determined at constant volume imply relative errors in the range 2–6%, except for k_2, which has an uncertainity of about 17%. Errors of this magnitude are higher than observed by a factor of 2 at most of the reaction temperatures. Relative parameter errors are a reflection of the magnitude of V_0, as indicated by the range for σ_α at 600 K given in Fig. 2. A typical regression map illustrating the parameter values obtained for each cycle of the iteration sequence for data collected at constant volume is given in Fig. 3. Figure 3 reveals that convergence became rapid after the third iteration, as indicated by the small changes in successive values of the parameters.

Rate parameters with standard deviations for the average at each reaction temperature are summarized in Tables 3 and 4. Standard deviations for the average values of k_1 and k_2 determined at constant volume in Table 3 were derived by error propagation [12] from the individual absolute errors de-

TABLE 3

Summary of kinetic parameters for decomposition of HNAB at constant volume from 560 to 633 K

Temp. (K)	M_0 (mg)	$M/V \times 10^2$ (mg mm^{-3})		$k_1 \times 10^4$ [a] (mg^{1-x} s^{-1})	$k_2 \times 10^6$ [a] (mg^{1-y-z} s^{-1})	x	y	z
633	4.24	28.3		26.82	1507	0.5071	0.5473	2.317
	2.52	16.8		48.50	293.4	0.6164	1.384	5.725
			av.	37.7 ± 1.24	900 ± 90.0	0.562 ± 0.0244	0.966 ± 0.0606	4.021 ± 0.171
6.23	4.64	30.9		40.25 ± 0.646	1296 ± 59.2	0.4538 ± 0.00691	0.7128 ± 0.0217	1.905 ± 0.0261
612	2.35	15.7		20.22 ± 0.718	549.5 ± 78.6	0.6901 ± 0.0258	1.843 ± 0.200	4.901 ± 0.371
600	4.13	42.2		16.77	193.5	0.5141	2.292	2.600
	2.52	16.8		15.68	81.97	0.6926	4.957	7.787
			av.	16.2 ± 0.2057	138 ± 17.3	0.603 ± 0.00682	3.62 ± 0.1026	5.19 ± 0.111
590	5.94	71.5		9.889	294.9	0.2851	1.596	1.845
	2.93	19.5		7.842	101.9	0.5870	3.286	4.614
			av.	8.87 ± 0.248	198 ± 9.85	0.436 ± 0.0264	2.44 ± 0.0766	3.23 ± 0.0996
580	2.98	19.9		6.886 ± 0.0268	22.64 ± 1.26	0.4787 ± 0.00311	4.866 ± 0.0768	5.965 ± 0.0782
570	9.02	60.1		3.011	36.92	0.3472	1.612	1.888
	3.65	24.3		4.695	8.977	0.3927	3.959	4.664
			av.	3.85 ± 0.0676	22.9 ± 1.47	0.370 ± 0.00985	2.79 ± 0.0464	3.28 ± 0.0379
560	9.23	61.5		4.074	6.381	0.2143	2.320	2.224
	2.89	19.3		1.671	86.22	0.2152	3.119	3.483
			av.	2.87 ± 0.0421	46.3 ± 1.081	0.215 ± 0.00475	2.72 ± 0.0255	2.85 ± 0.0272

[a] Average errors correspond to one σ derived from error propagation assuming $k = \Sigma k_i / N$.

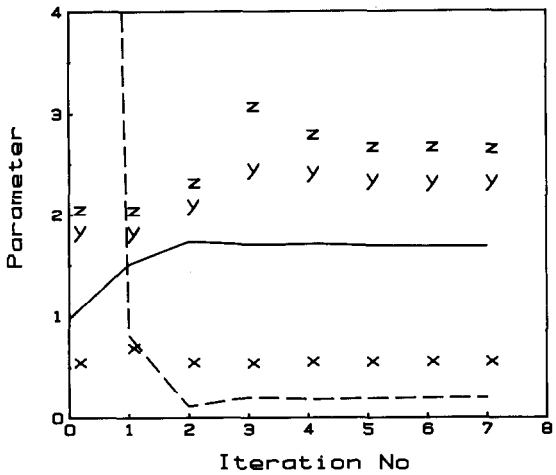

Fig. 3. Regression map for HNAB decomposition at constant volume, 600 K: ——, $k_1 \times 1000$; - - - - - -, $k_2 \times 1000$.

termined for each run at each reaction temperature. Errors for data evaluated at constant pressure correspond to the overall standard deviation based on the assumption of a unit weight for each observation. Although data for k_1 are essentially independent of sample mass and the M/V ratio, the data for k_2 indicate a significant dependence upon both M/V at constant volume and sample mass at constant pressure. The variations of k_2 with crucible free volume and sample mass are similar to results reported for other secondary explosives [13].

A plot of the reaction order x and the ratio, $y/(y+z)$ over the range 580–610 K determined from the constant pressure data tabulated in Table 4 is illustrated in Fig. 4. The magnitude of x varies from 0.58 to 0.74 over the whole temperature range, while $y/(y+z)$ tends to decrease at higher temperatures. The decrease of $y/(y+z)$ with temperature is an indication of a change in mechanism and a reduced contribution from reactions associated with the autocatalytic transition. Individual values of y and z at a given temperature determined at constant volume varied by a factor as high as three (compare data at 600 K in Table 3) for a two- to three-fold change in the M/V ratio and tended to decrease with a reduction of the crucible free volume. Thus, a unique set of parameters for y and z could not be determined at constant volume. These results indicate that HNAB decomposition is sensitive to pressure perturbations associated with the heterogeneous reactions of the autocatalytic transition. Comparisons of the calculated and experimental thermograms for constant volume at 590 and 600 K are illustrated in Fig. 5.

A plot of the standard residuals, $(P_i - P_{\text{calc}})/\sigma$, [14] versus time, for each thermogram, is illustrated in Fig. 6.

TABLE 4

Summary of kinetic parameters for decomposition of HNAB at constant pressure [a] from 580 to 610 K

Temp. (K)	M_o (mg)		$k_1 \times 10^5$ ($mg^{1-x}\ s^{-1}$)	$k_2 \times 10^6$ ($mg^{1-y-z}\ s^{-1}$)	x	y	z
610	6.63		250.5	8.183	0.7433	2.540	3.903
	5.12		332.1	129.6	0.6893	1.288	3.572
	3.45		252.4	103.61	0.7952	2.455	4.939
		av.	278 ± 46.7	80.5 ± 63.9	0.743 ± 0.0530	2.094 ± 0.700	4.14 ± 0.713
600	11.47		227.5	25.13	0.6648	1.544	2.659
	9.72		176.8	24.25	0.6830	1.827	2.843
	8.31		223.2	41.41	0.5680	1.711	2.724
	6.72		232.2	20.17	0.6322	2.264	3.219
		av.	215 ± 11.9	27.7 ± 9.37	0.637 ± 0.0506	1.84 ± 0.3078	2.86 ± 0.2504
590	12.85		145.0	10.66	0.7240	2.852	2.751
	11.18		115.4	12.37	0.7361	2.051	2.491
	8.96		135.5	31.03	0.6728	2.674	3.214
	8.46		155.8	18.85	0.5901	2.995	3.305
	5.88		122.9	35.52	0.5876	2.198	3.076
	3.78		140.8	10.76	0.6519	1.606	2.242
		av.	136 ± 14.8	19.9 ± 10.9	0.660 ± 0.0636	2.40 ± 0.534	2.85 ± 0.424
580	11.09		134.6	11.47	0.6233	2.032	2.534
	9.88		98.13	29.86	0.7277	1.540	2.672
	9.70		108.2	4.299	0.5801	2.407	2.849
	9.14		104.9	14.33	0.6251	2.242	2.447
	7.46		94.96	9.592	0.5067	2.362	3.054
	6.94		94.64	23.82	0.5073	2.130	2.857
	4.07		71.70	40.37	0.5109	2.630	3.920
		av.	101 ± 18.9	19.1 ± 12.8	0.583 ± 0.0828	2.19 ± 0.347	2.904 ± 0.493

[a] Crucible buffer volume ≈ 500 cm^3, $P = 5 \times 10^6$ Pa.

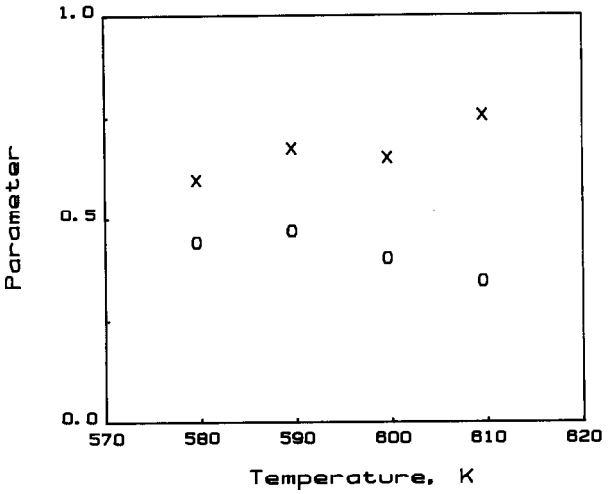

Fig. 4. Variation of x and $y/(y+z)$ with temperature for HNAB decomposition at constant pressure; O, y/($y+z$).

Arrhenius parameters were determined by regression on the converged values of the rate coefficients, and the results are summarized in Table 5. In order to insure the correct standard deviation for the Arrhenius parameters, each observation was weighted as $(2.303k_i/\sigma_i)^2$ [15]. Arrhenius plots for k_1 and k_2 illustrating the regression fits at constant volume and constant pressure are given in Figs. 7 and 8.

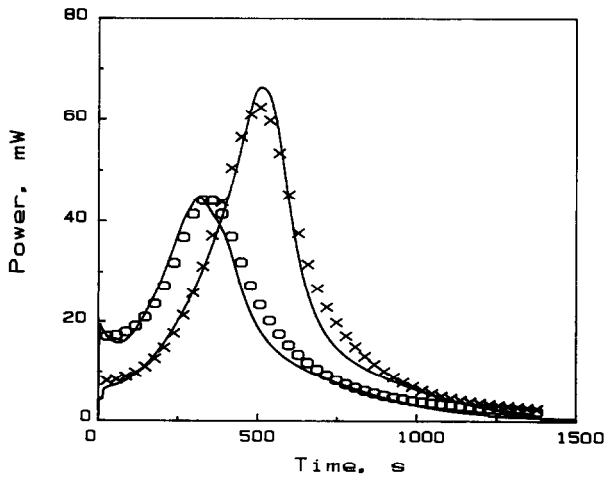

Fig. 5. Calculated and experimental thermograms for HNAB decomposition at constant volume: ×, 5.94 mg, 590 K; O, 4.13 mg, 600 K; ———, expt.

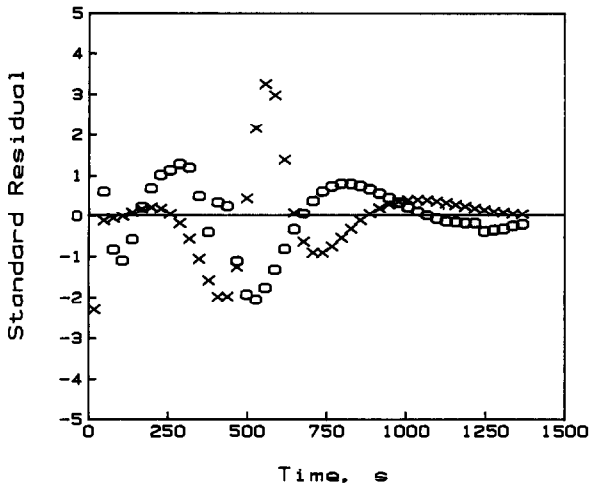

Fig. 6. Variation of standard residuals with time for HNAB decomposition at constant volume: ×, 590 K, $\sigma = 3$ mW; ○, 600 K, $\sigma = 1$ mW.

TABLE 5

Arrhenius parameters for decomposition of HNAB over the temperature range 560–633 K

Transition	log A [a,b]	E [b] (kJ mol^{-1})
1	7.48 ± 0.47 [c]	118 ± 5.3 [c]
	6.04 ± 0.78 [d]	100 ± 9.1 [d]
2	8.92 ± 2.67 [c]	143 ± 29.5 [c]
	11.2 ± 4.01 [d]	178 ± 46.6 [d]

[a] Units for A are mg$^{1-x_s-1}$ and mg$^{1-y-z_s-1}$ for transitions 1 and 2, respectively.
[b] Errors correspond to one σ.
[c] Const. V, statistically weighted.
[d] Const. P, unit weighted.

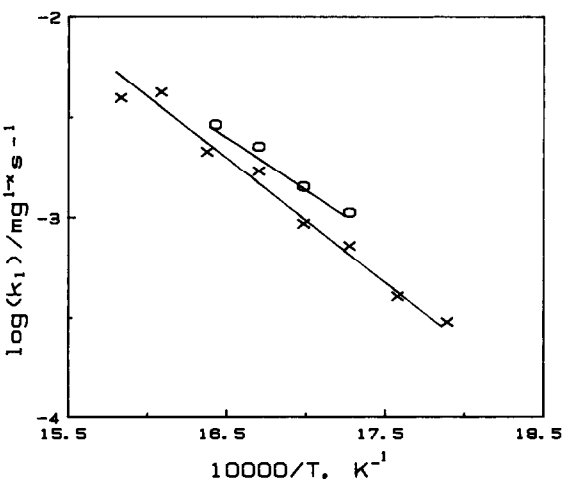

Fig. 7. Arrhenius plots for transition 1 from 560 to 633 K: ×, const. V; ○, const. P.

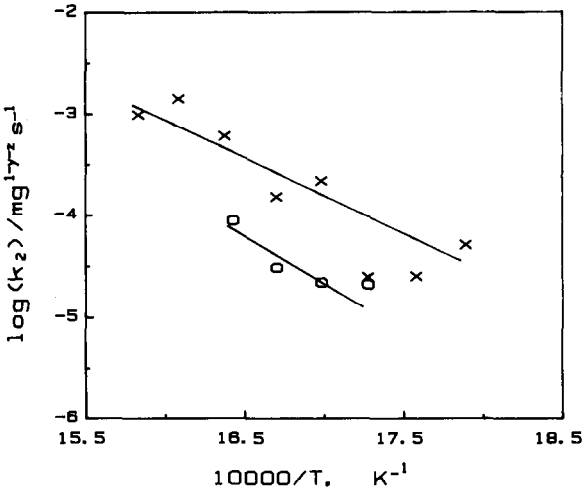

Fig. 8. Arrhenius plots for transition 2 from 560 to 633 K: ×, const. V; ○, const. P.

CONCLUSIONS

The objective of this work was to devise a reliable method to evaluate global rate parameters from DSC reactivity curves for condensed phase reactions. Application of the regression for more complex systems requiring additional parameters is easily implemented; sums of the products of the partial derivatives for additional parameters are simply added to the left hand side of the system of linear equations given in eqn. (4). However, the potential for an ill-conditioned and divergent coefficient matrix increases as the number of undetermined parameters increases.

Comparisons of the calculated and experimental thermograms in Fig. 5 suggests that the residuals vary in a periodic manner with alternating blocks of plus and minus values. This is particularly evident for the curve at 590 K for the calculated data points in the range 600–800 s. In the absence of systematic errors, non-random variations of the residuals indicate that the regression function does not adequately describe the data [8,14]. However, the overall standard deviations for the plots in Fig. 5 and 590 and 600 K are 1 and 3 mW respectively. All of the points in the standard residual plots given in Fig. 6 are within one standard deviation, except for a few points in the range 500–700 s; therefore, the regression fits are satisfactory. For decomposition of HNAB, the alternating character of the residuals probably arises from systematic errors associated with the heterogeneous reactions of the autocatalytic transition.

The consistency between the data for k_1 at both constant volume and constant pressure given in Fig. 7 suggests that the first transition is essentially independent of pressure and/or crucible free volume. The activation energy, $E_1 = 118 \pm 5.3$ kJ mol^{-1} for k_1 compares favorably with a value of

122 kJ mol^{-1} [16–18] determined from initial rates of gas evolution. Conceptually, the autocatalytic transition arises primarily from sums of elementary transfer and radical-addition reactions with expected activation energies in the range 25–60 kJ mol^{-1} [10,11,19]. Error propagation is additive for a series of competing reactions; therefore, the large standard deviation determined for E_2 of the autocatalytic transition was not totally unexpected. Significant reductions in systematic error and relative errors observed for k_2 could be achieved if data were collected at constant pressure under conditions of minimum crucible free volume. Such an approach would improve the precision of the Arrhenius parameters calculated for the autocatalytic transition. Unfortunately, minimization of the crucible free volume for explosives decomposition is difficult to achieve without accompanying sample deflagration and/or thermal explosion.

Reliable Arrhenius parameters are required to correctly predict the critical ignition temperatures of explosives subjected to specific geometric and boundary constraints [20,21]. Uncertainty in calculated the Arrhenius parameters arising from systematic errors and the additive nature of error propagation for competing reactions may, in part, account for the large discrepancy between the calculated and experimental critical ignition temperatures [22] determined for the explosive, HNAB.

ACKNOWLEDGMENT

This work was sponsored by the U.S. Department of Energy under Contract No. DE-AC04-76-DP43495.

REFERENCES

1 J.M. Pickard, Proc. of the 17th North American Thermal Analysis Society Meeting, October 13–15, 1988, Lake Buena Vista, FL, Vol. 2, p. 701.
2 E. Koch, Non-Isothermal Reaction Analysis, Academic Press, London, 1977, p. 91.
3 R.N. Rogers, Thermochim. Acta, 3 (1972) 437.
4 R.N. Rogers, Anal. Chem., 44 (1972) 1336.
5 A. Dutta and M.E. Ryan, J. Appl. Polym. Sci., 24 (1979) 635.
6 R.N. Rogers and J.L. Janney, Proc. of the 11th North American Thermal Analysis Society Conference, October 13–15, 1981, New Orleans, LA, Vol. 2, p. 643.
7 M.R. Kennan, Proceedings of the Eighteenth International SAMPE Technical Conference, October 13–15, 1986, Seattle, WA, Vol. 18, p. 841.
8 W.E. Wentworth, J. Chem. Ed., 42 (1965) 96.
9 W.E. Wentworth, J. Chem. Ed., 42 (1965) 162.
10 I. Oref and A. Leiba, J. Chem. Soc. Faraday Trans., 75 (1979) 2694.
11 D. Barton, M. Hodgett, P. Skirving, M. Whelton, K. Winter and C. Vardy, Can. J. Chem., 61 (1983) 1712.
12 A.C. Norris, Computational Chemistry, John Wiley and Sons, New York, 1981, p. 50.

13 R.N. Rogers and G.W. Daube, Anal. Chem., 45 (1973) 596.
14 J.F. Rusling, J. Chem. Ed., 65 (1988) 863.
15 A.C. Norris, Computational Chemistry, John Wiley and Sons, New York, 1981, p. 195.
16 Y.Y. Maksimov and L.A. Shipicin, Prikl. Geofiz, 73 (1974) 195.
17 Y.Y. Maksimov and E.N. Kogut, Khim. Khim. Tekhnol., 20 (1977) 349.
18 S. Zeman, Thermochim. Acta, 31 (1979) 269.
19 S.W. Benson, Thermochemical Kinetics, John Wiley and Sons, New York, 1968, pp. 101, 106.
20 R.N. Rogers, Thermochim. Acta, 11 (1975) 131.
21 J.M. Pickard, J. Hazard, Mater., 9 (1984) 121.
22 J.M. Pickard, unpublished data.